frontiers | Frontiers in Earth Science

TYPE Original Research
PUBLISHED 29 September 2022
DOI 10.3389/feart.2022.1005199

OPEN ACCESS

EDITED BY
Huokun Li,
Nanchang University, China

REVIEWED BY
Yankun Wang,
Yangtze University, China
Xiaojun Su,
Lanzhou University, China

*CORRESPONDENCE
Jun He,
202111601003@stu.hebut.edu.cn

SPECIALTY SECTION
This article was submitted to Geohazards and Georisks, a section of the journal Frontiers in Earth Science

RECEIVED 28 July 2022
ACCEPTED 08 September 2022
PUBLISHED 29 September 2022

CITATION
Qin H, He J, Guo J and Cai L (2022), Developmental characteristics of rainfall-induced landslides from 1999 to 2016 in Wenzhou City of China. *Front. Earth Sci.* 10:1005199. doi: 10.3389/feart.2022.1005199

Developmental characteristics of rainfall-induced landslides from 1999 to 2016 in Wenzhou City of China

Haiyan Qin[1], Jun He[2]*, Jian Guo[3] and Lu Cai[3]

[1]The Eleventh Geological Brigade of Zhejiang Province, Wenzhou, China, [2]School of Civil and Transportation Engineering, Hebei University of Technology, Tianjin, China, [3]Zhoushan SLT Ocean Technology Co., Ltd., Zhoushan, China

Many landslides are triggered by excess precipitation. In the eastern part of China, landslides caused by extreme rainfall from typhoons in the monsoon season are the main geomorphological process with catastrophic impacts on society and the environment. In this study, Wenzhou City in eastern China was taken as the study area, and we compiled a detailed inventory of rainfall-triggered landslides between 1999 and 2016. The developmental characteristics of these landslides were determined with an emphasis on temporo-spatial distribution. The results showed that most of the landslides were located in the mountainous area of the western part of Wenzhou City. Landslides triggered by typhoon rainfall were commonly concentrated in a short period from July to September, when more than 70% of the landslides occurred. The landslides in this region were mainly of the debris-flow type, most of which were on a small scale, but had severe effects because of large elevation differences and long runout distances. Because the precipitation in typhoon events was commonly extreme, the initiation area of most landslides coincided with the region of highest hourly precipitation. Our results can provide reference data and guidelines for developing an early warning system for landslides and risk reduction in the study area.

KEYWORDS

rainfall-induced landslide, temporo-spatial characteristics, development laws, typhoon, China

1 Introduction

It is well known that East Asia is one of the main areas suffering from rainfall-induced landslides due to the onset and duration of the monsoon (Wu et al., 2014; Guo et al., 2019; Guo et al., 2020). Statistical data showed that China suffers from more than 10% of all rainfall-triggered landslide events worldwide (Froude and Petley, 2018). One important characteristic of the Asian monsoon is the typhoon (Webster et al., 1998), which commonly causes very heavy precipitation that can trigger cluster landslides in the hilly coastal region (Zhuang et al., 2022). In eastern China, typhoon rainfall-triggered landslides are major geomorphological activities, causing damage to infrastructure and

the environment each year to the extent of millions of RMB (Wang and Yin 2018; Zhou et al., 2020; Li et al., 2021). Hence, it is of great importance to determine the developmental mechanisms behind these landslides for both the scientific community and local authorities.

Regional landslides triggered by extreme rainfall events generally occurred in clusters (Medina et al., 2021; Hürlimann et al., 2022), so understanding the mechanism and assessment of landslide episodes relies on the availability of landslide inventories (Crozier, 2005; Wu et al., 2020; Guo C et al., 2021). Creation of a landslide inventory is the first step toward understanding landslide susceptibility, hazard, and risk assessment (Guzzetti et al., 1999; Fell et al., 2008; Huang F. et al., 2021). Manual techniques have been widely applied to compile landslide inventories across large areas, but they are time-consuming, difficult in practice, and sometimes not suitable for mountainous terrains or highly concentrated landslides (Santangelo et al., 2010). To overcome these drawbacks, some advanced approaches and tools have been developed to map landslides semi-automatically or automatically to produce an inventory. For instance, algorithms based on different sources such as satellite data, interferometric synthetic aperture radar (InSAR) technology, and unmanned aerial vehicle (UAV) photogrammetry (Alvioli et al., 2018; Prakash et al., 2020; Abancó et al., 2021; Guo Z et al., 2021). However, the most widely accepted methods so far are hybrid ones that balance accuracy and efficiency. For example, Hürlimann et al. (2022) created a detailed inventory of landslides triggered by extreme rainfall events in the Pyrenees in 2013 by interpretation of aerial photographs, helicopter flights, and field surveys.

It is widely accepted that future climate change combined with more extreme rainfall events will increase the frequency and magnitude of rainfall-induced landslides in mountainous areas (Huang et al., 2022a; Yin et al., 2022). Besides being affected by the monsoon climate, the eastern part of China often suffers from heavy precipitation in the rainy season every year. Due to the hydrological effect induced by heavy rainfall, the soil pore pressure and effective stress decrease (Jiang et al., 2018; Huang et al., 2022b), which rapidly increases the risk of slope failure. Thus, considering the relationship between a rainfall-induced landslide inventory and extreme rainfall facilitates the analysis of landslide risk. The eastern part of China often suffers from heavy precipitation in the monsoon season every year; however, most such studies focused on regional landslide hazard assessment (including susceptibility analysis) (Liu et al., 2012; Wang and Yin, 2018; Huang et al., 2020), rainfall threshold definition (Chang et al., 2008; Ma et al., 2015; Wei et al., 2017), and implementation of an early warning system (Wu et al., 2014; Wei et al., 2018). Only a limited number of reports have been published investigating the geophysical laws and characteristics of these rainfall-induced landslides, although this should be a foundational step for landslide hazard assessment. For example, Jia et al. (2019) collected the geohazards in Zhejiang province, China, from 2000 to 2016 and summarized the number of landslides and their damages, but the analysis of landslide characteristics was missing. Based on landslide monitoring during 72 h of rainfall before the landslide occurrence, Kim et al. (2021) determined an empirical threshold, but did not consider the event a result of rainfall on the shallow landslide.

In this study, Wenzhou City in eastern China was selected as the study area, and our main objectives included: (1) creating a rainfall-induced landslide inventory from 1999 to 2016, (2) analyzing the temporal and spatial distribution characteristics of these landslides, and (3) revealing other properties coinciding with landslide occurrence.

2 Study area

2.1 General settings

The study zone encompassed Wenzhou City (N 27°03′, E 119°37′~N 28°36′, E 121°18′) in southeastern China, with a total area of 12,110 km^2 (Figure 1). The area is part of the mountainous region in the Yangtze River valley belt in southern Zhejiang province. It is characterized by a landscape of mountains, hills, and coastal plains. The elevation in the region ranges from 120 to 1656 m above sea level (asl), and overall the northwest part is higher than the southeast part. Except for inter-mountain basins and river valleys, the major topographical feature in this area is the large elevation difference (topographic relief) (Zhang et al., 2014; Wang and Yin 2018). With respect to the geological setting, a total of four strata are observed including Late Yanshanian, Cretaceous, Jurassic, and Quaternary. Most of these geologic units have a sub-horizontal layering and several vertical sets of subunits. The most important difference among these strata is the lithology, with sedimentary rock, pyroclastic rock, and intrusive rock being the most common in the area. The Quaternary is represented by colluvial deposits, which cover the bedrock in the eastern part of the region.

Wenzhou City has a subtropical monsoon climate with a mean temperature ranging from 17.3°C to 19.4°C and an average annual rainfall of 1500 to 2000 mm. There is a clear temporal difference in rainfall pattern: the rainy season normally lasts from May to September, and the highest total precipitation occurs between June and August because of typhoons (Liu et al., 2010; Liu et al., 2011).

The resident population of the region is approximately 9.6 million and the settlements are mainly distributed in the eastern part. The banks of the Yangtze River are especially highly populated and urbanized.

2.2 Materials and data

A landslide inventory can reveal the spatial distribution of landslides in a visible form and store basic landslide information

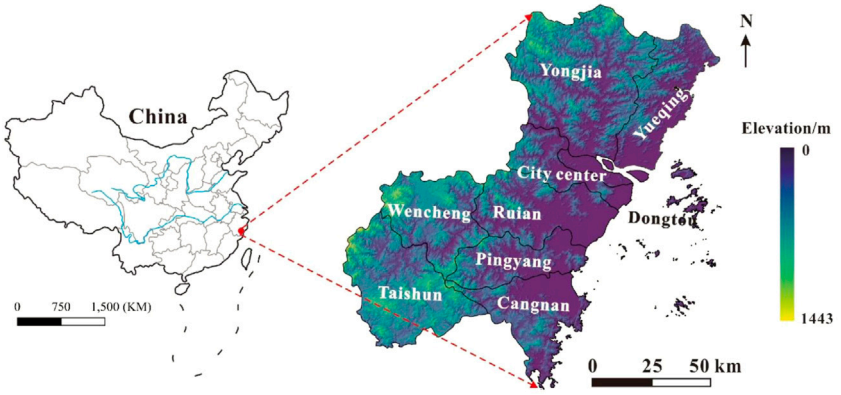

FIGURE 1
Location of the study area where the base map is the DEM of the region with 30-m resolution and shows the distribution of administration areas.

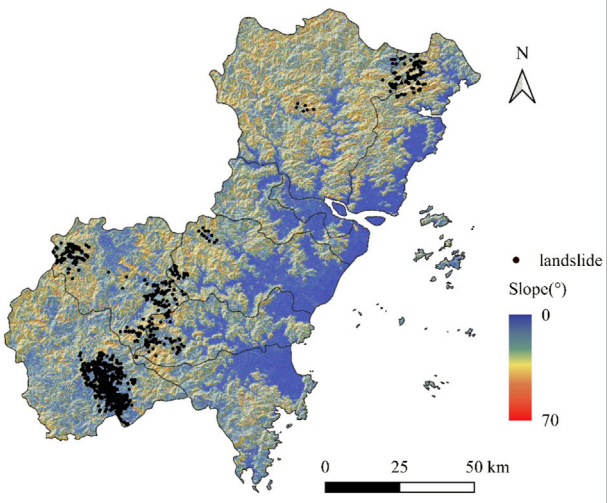

FIGURE 2
Distribution of landslides in the inventory of Wenzhou City. The base map is the slope map with 30-m resolution.

(Peng et al., 2019; Huang Y. et al., 2021), hence it is the foundation for the analysis of the development characteristics of regional landslides. In this study, archived landslide reports were provided by a local geo-environmental monitoring institution in which the coordinates of rainfall-induced landslides were recorded. Then Google Earth images were combined with landslide reports to generate a coarse landslide inventory. To check and update the accuracy of the locations of these landslides, a field survey and indoor cross-validation were conducted by the Geological Exploration Bureau of Zhejiang province in 2016. During the fieldwork, advanced equipment including drones, handheld global position system (GPS) devices, and infrared range finders were used to measure and record basic landslide information. Subsequently, all of the archived data from the fieldwork were compared with the images to determine the landslide initiation area. In the last step, the distribution of these landslides was digitized into a geographic information system (GIS) along with their properties, including the area, volume, temporal information, width, length, and damage caused.

The digital elevation model (DEM) data of the region was downloaded from the free Geospatial Data Cloud website (https://www.gscloud.cn/home). Some environmental factors can be generated from the DEM, such as slope and curvature, which can be used for the analysis of the conditioning factors of the landslides. The landslide inventory listed a total of 1450 landslides, which were associated with eight typhoon events (Figure 2), including the flood in 1999, typhoon Rananim in 2004, typhoon Talim in 2005, typhoon Fitow in 2013, typhoon Soudelor in 2015, typhoon Soudelor in 2015, typhoon Meranti in 2016, typhoon Megi in 2016, and typhoon Haima in 2016. According to widely accepted classification criteria (Varnes 1978; Hungr et al., 2014), these landslides can be divided into three types: (1) debris flow, which accounts for more than 80% of the landslides, (2) debris slide, and (3) earthflow related to top soil layers. Based on the inventory, the developmental characteristics of the rainfall-induced landslides were determined.

3 Results

3.1 Temporal characteristics

The temporal characteristics of the landslides in the study area are mainly related to the temporal distribution of rainfall. Figure 3A, shows the distribution of the number of days with heavy rainfall events during the 42 years from 1972 to 2013. We defined heavy rainfall as daily precipitation >30 mm (Khan et al., 2012; Robbins 2016), which concurs with the criteria of the China Meteorological

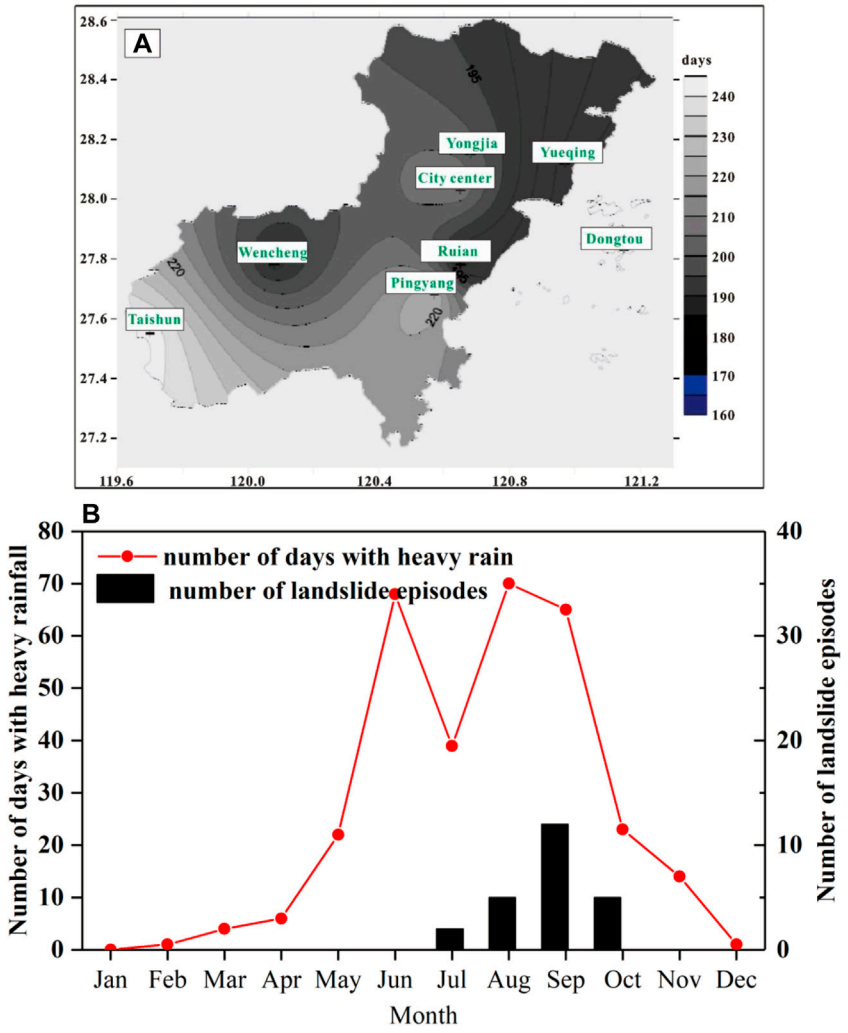

FIGURE 3
Relationship between landslides and rainfall in the study area: **(A)** spatial distribution of the number of days with heavy rainfall events during 1972 and 2013 in Wenzhou City, and **(B)** relationship between the number of days with heavy rainfall and the number of landslide episodes in each month.

Administration. It is evident that the southwestern part has more heavy rainfall events than the northeastern part. If the monthly distribution is considered, it can be seen that most heavy rainfall events happen between June and October, which corresponds to the occurrence of high-density landslides during a short time that only occur from June to October (Figure 3B). Hence, summer and autumn are the times of the highest rainfall-induced landslide risks in the region, which can be explained as a result of the impact of the Asia monsoon. For example, the landslide episode triggered by typhoon Rananim in 2004 occurred during the period with the highest intensity (Figure 4). Similar results can also be observed from the landslide episodes triggered by other typhoon events. Hence, from the frequent occurrence of landslides on steep slopes it can be inferred that the study area responded quickly to high-intensity rainfall. The time interval between landslide occurrence and peak precipitation during the typhoon event was commonly from 30 to 60 minutes. This fits well with the field survey results: the Baofeng debris flow in Wencheng County occurred ~10 min after typhoon Megi in 2016 and the Cangjiang landslide occurred only 5 min after typhoon Soudelor in August 2015. This association occurs because heavy rainfall can make the soil layer saturated for a short time (Kuradusenge et al., 2021), then the continuing rainfall generates large runoff that provides enough excitation energy to cause the movement of rock-soil masses.

3.2 Spatial characteristics

Overall, the landslide distribution of Wenzhou City is spatially heterogeneous. Rainfall-induced landslides are mainly

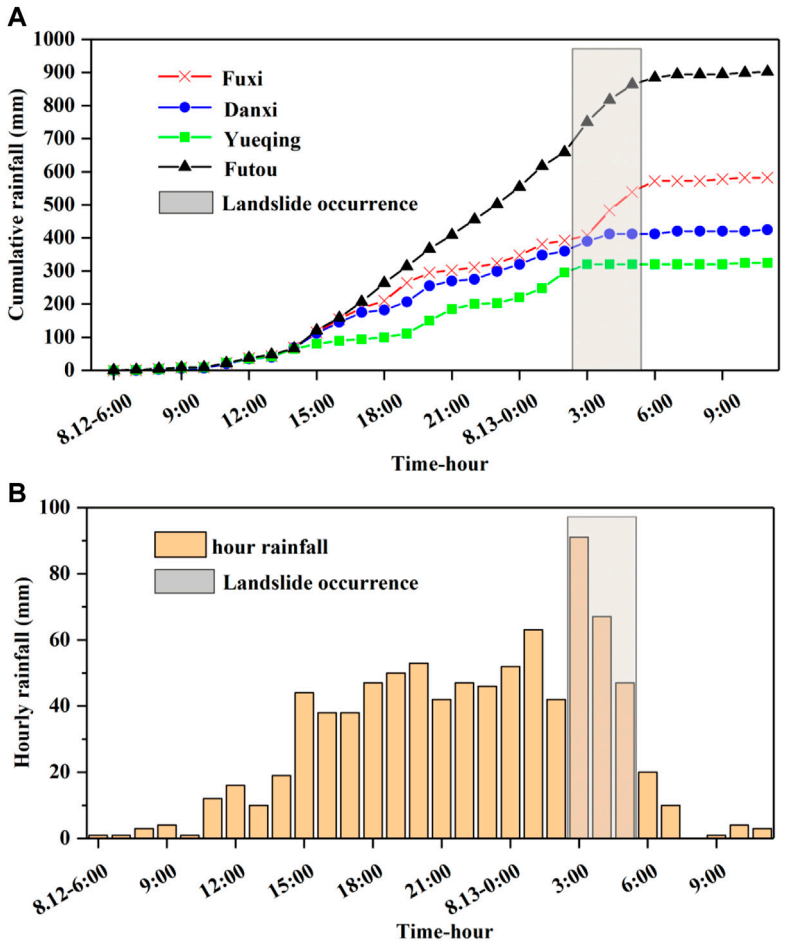

FIGURE 4
Cumulative rainfall and hourly rainfall intensity during typhoon Rananim in 2004. **(A)** Cumulative rainfall recorded by four different monitoring stations and **(B)** hourly rainfall in the Fuxi monitoring station.

distributed in the western part of the region, which includes the mountainous areas of Yueqing, Yongjia, Wencheng, Taishun, etc. On the contrary, the eastern part of the region, including Dongtou, Pingyang, and Cangnan, with lower elevation and gentle topography recorded few landslides. When we analyzed the distribution of landslides triggered by a single typhoon event is, we found that the landslide locations had a close relationship with the moving path of the typhoon. The area with the highest landslide density was commonly the region that had the heaviest rainfall or the greatest rainfall intensity. For example, typhoon Haima triggered 36 landslides in 2016, most of which were located in the area with the largest accumulated precipitation according to the rainfall isohyetal map. The relationship between landslide distribution and elevation was also analyzed, and the results showed that 4.84% of the landslides occurred in areas with elevations <100 m, where the topography is mainly eroded and denuded hills. In contrast, 13.41% of the landslides were located in areas with elevations between 100 and 400 m. Landslides at elevations of 400 to 700 m and 700 to 1000 m accounted for 34.59% and 43.38%, respectively, whereas only 3.78% of landslides are at elevations >1,000 m (Figure 5A). With regard to the elevation difference between the initiation area and the accumulation area, most landslides have elevation differences of <100 m, accounting for 43.94% of all landslides, whereas 21.31% of landslides have elevation differences of >200 m (Figure 5B). Geomorphology also had an impact on landslide occurrence. Statistical testing revealed that 56.61% of the landslides were significantly located near the top of a mountain or on flat areas of steep slopes. Concave curvature developed in 24.74% of the landslides, and the landslides below the cliff accounted for 18.65%. Hence, mountainous areas were the most important topography for rainfall-induced landslides in Wenzhou City.

Due to the rainfall distribution affects on landslide occurrence, it is common in this region for landslide density to be especially high in certain areas. Table 1 reveals the density of

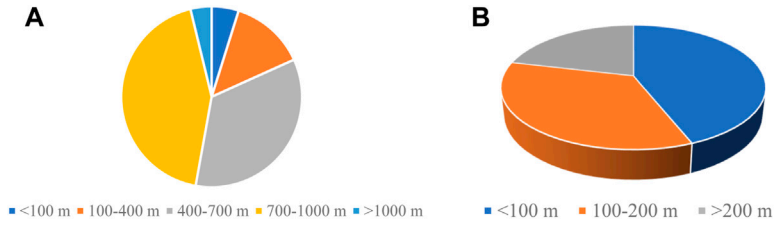

FIGURE 5
Relationship between landslide distribution, elevation, and elevation difference. **(A)** Elevation of initiation area and **(B)** elevation difference between initiation and accumulation areas.

TABLE 1 Statistics on density and duration of typhoon-triggered landslides in the region.

Typhoon	Flood	Rananim	Talim	Soudelor	Meranti	Megi	Haima
The area most affected by landslides	Yongjia	Yueqing	Wencheng	Wencheng	Taishun	Wencheng	Ruian
Landslide density	0.5/km^2	0.65/km^2	1.21/km^2	0.8/km^2	3.69/km^2	0.87/km^2	6.4/km^2
The duration of the landslide episode	1 h	2 h	1 h	1 h	2 h	2 h	1 h

landslide episodes triggered by different typhoon events between 1999 and 2016. It can be seen that although the period is quite long, most landslides occurred only for a few days, which meant that the overall stability conditions in the region were good in the absence of excessive precipitation. For example, typhoon Haima triggered more than 200 landslides, a high density of 6.4/km^2, but only for a few hours. The number of landslides in that single event comprises more than 70% of the rainfall-triggered landslides in the region over the past 30 years. Moreover, because typhoon rainfall often shows a peak value in a small area, which is significantly higher than in other regions, landslides triggered by such an event are mostly distributed only in this small region (Dahal et al., 2009; Nolasco-Javier et al., 2015). Thus, typhoon Haima only caused slope failure in Ruian County because this region had the highest rainfall (Table 1).

3.3 Other characteristics during landslide occurrences

3.3.1 Small-scale landslides with severe damage

According to available data on volumes of rainfall-induced landslides, more than 80% of landslides in the region were characterized as small-scale in volume (less than 10^4 m^3). The average duration of a landslide was 10 to 20 min and the mean width was between 5 and 10 m. The rainfall-induced landslide with the largest volume so far was the debris-flow event in Yongjia in September 1999, which had a volume of 2×10^5 m^3 (Figure 6). However, rainfall-induced debris flows mostly occurred in the middle and upper parts of steep slopes. Under these conditions, there was considerable potential energy because of the large height difference between the initiation area and the bottom of the channel. The debris-flow moved downwards rapidly from the high initiation site under the action of potential energy and mixed with a large amount of rock, soil, and vegetation to form a heavy debris flow in the channel, destroying vegetation, buildings, and other structures along the way. Because of the large amount of precipitation, the run-out distance and velocity in the channel may also be large, which poses a dangerous hazard to residents and properties. For example, on 1 September 2005, under the influence of typhoon Talim, a debris flow with an area of ~3000 m^3 occurred in Shimen Village of Wencheng County, which caused five deaths, two injuries, and damaged seven houses. The total direct economic loss caused by this damage exceeded one million RMB. The total run-out distance of this debris flow was approximately 1 km, during which the maximum velocity reached ~3 m/s.

3.3.2 Disaster chain reactions

According to filed surveys and detailed landslide reports provided by local authorities, we found that the geohazards in the study area showed obvious disaster chain reactions, which means that landslides generally occur together with other kinds of disasters. For example, extreme rainfall causes flooding as well as landslides. The slope instability provides material sources, which can trigger debris flow in the channel by combining with floodwaters. A typical disaster chain triggered by heavy rainfall in the study area mainly included three types: (1) debris flow in the channel due to landslide initiation, (2) Earth flow along the slope surface caused by slope instability (Figure 7A), and (3) a debris flow that slides into a river causing a tsunami and landslide dam (Figure 7B).

FIGURE 6
Debris flow occurrence in September 1999 in Yongjia of Wenzhou.

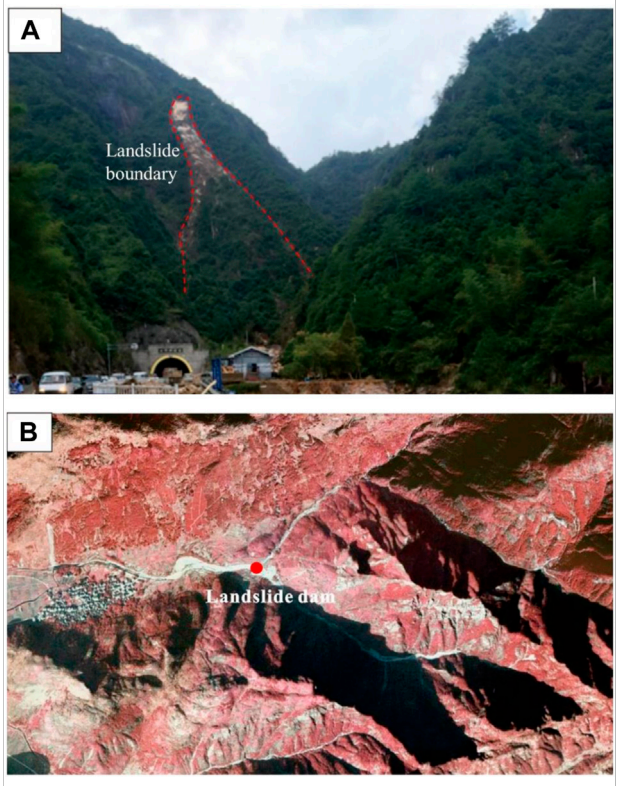

FIGURE 7
Two types of disaster chain in the study area. **(A)** Earth flow on the slope surface from slope instability and **(B)** landslide dam caused by debris flow into a river.

4 Discussion

In this study, a detailed typhoon rainfall-triggered landslide inventory was obtained by manual visual interpretation of remote-sensing images and fieldwork. Seven typical typhoon events in the past 17 years have caused serious landslide disasters. The temporo-spatial landslide inventory characteristics indicated that the prevalence of typhoon rainfall-triggered landslides in the area was highly consistent with the distribution of rainfall intensity, and events were clustered in hilly areas. The spatial characteristics of the topography were strongly correlated with the probability that a landslide would occur. The hilly area in the western part of the study area proved to be a hotspot for the occurrence of rainfall landslides. It can be seen in Figure 2 that the landslides were mainly concentrated in the western mountainous part of the study area, while almost no landslides occurred in the flat terrain along the eastern coast even though it experienced the same typhoon events. In addition, sloping terrain facilitated the convergence of rainfall, making landslides more likely.

An interesting phenomenon during typhoon rainfall is the short lag time of typhoon rainfall-triggered landslides. According to the research of Naidu et al. (2018) and Medina et al. (2021), the antecedent rainfall has a great influence on the stability of shallow landslides. Through many field tests and numerical simulations, it was shown that this hydrological effect could greatly decrease soil pore pressure and effective stresses (Rahardjo et al., 2008; Rahimi et al., 2011). Because of the Asian monsoon climate, the typhoon-prone season in the study area coincided with the local rainy season to a large extent. This meant that the study area experienced heavy rainfall before the onset of typhoon rainfall. The infiltration of a large amount of rainfall greatly replenishes the groundwater, and the soil moisture content was relatively high during this period (Wang et al., 2017; Yin et al., 2022). Therefore, a large rainfall event caused the slip surface to saturate in a relatively short period of time (Xu et al., 2016), and the slope may fail in the short-term under typhoon-related heavy rains.

Due to the limitations of landslide inventory production, it is difficult to determine the specific time that a landslide occurred. Further analysis based on a process-based approach to establish a reliable and robust relationship between hourly

rainfall intensity and duration and the occurrence of landslides has been limited (Gabet et al., 2004). Considering the difficulty of obtaining detailed rainfall data on a regional scale, the resolution of rainfall data in this study was days. But, more detailed rainfall data with higher resolution such as hourly rainfall data would be more helpful for analyzing the occurrence of rainfall-induced landslides (Kirschbaum et al., 2009). Hence, considering the application of remote sensing rainfall instruments with various multitemporal and spatial resolutions in the future has excellent prospects for identifying rainfall-induced landslide characteristics (Kocaman et al., 2020; Tseng et al., 2020).

5 Conclusion

Rainfall-triggered landslides are the most important geohazard in the Zhejiang province of China. This study generated a landslide inventory that revealed for the first time the landslides triggered by typhoon rainfall events between 1999 and 2016 in Wenzhou City of Zhejiang province. Among the total 1450 landslides, more than 80% were debris flows. The landslide distribution was spatially heterogeneous with most landslides occurring in the western part of the region, which has a higher elevation than the eastern part. Landslides located in the area with elevations ranging from 400 to 1000 m comprised 77.97% of the total, and more than 55% of landslides occurred at elevation differences larger than 100 m. More than 70% of landslides occurred during the period from July to September due to the rainy season related to the Asia monsoon. Although the majority of landslides had small volumes in the range of hundreds of cubic meters, the damage caused may be greater because of large elevation differences and long run-out distances. Because precipitation during a typhoon is commonly extreme, the initiation area of most landslides coincided with the region of highest hourly precipitation along the typhoon's path. Moreover, the disaster chain effect is another characteristic of landslides in Wenzhou City, where landslides commonly occurred together with other disasters resulting in greater harm to residents and damage to property. Our results contribute to the understanding of the mechanisms of regional rainfall-induced landslides and also can provide references and guidelines for developing early warnings for imminent landslide potential and risk reduction in similar contexts.

Data availability statement

The original contributions presented in the study are included in the article/Supplementary Material, and further inquiries can be directed to the corresponding author.

Author contributions

HQ: conceptualization, methodology, investigation, datacuration, formal analysis, and writing the original draft. JH: conceptualization, validation, and reviewing and editing thepaper. JG: data curation, reviewing and editing the paper. LC: reviewing and editing the paper.

Funding

This study was funded by the Bureau of Land and Resources of Wenzhou project (Wentuzi (2016) no. 89).

Acknowledgments

JH wants to thank the Eleventh Geological Brigade of Zhejiang Province for providing the field survey data.

Conflict of interest

JG and LC were employed by Zhoushan SLT Ocean Technology Co., Ltd.

The remaining authors declare that the research was conducted in the absence of any commercial or financial relationships that could be construed as a potential conflict of interest.

Publisher's note

All claims expressed in this article are solely those of the authors and do not necessarily represent those of their affiliated organizations, or those of the publisher, the editors and the reviewers. Any product that may be evaluated in this article, or claim that may be made by its manufacturer, is not guaranteed or endorsed by the publisher.

References

Abancó, C., Bennett, G. L., Matthews, A. J., Matera, M. A. M., and Tan, F. J. (2021). The role of geomorphology, rainfall and soil moisture in the occurrence of landslides triggered by 2018 Typhoon Mangkhut in the Philippines. *Nat. Hazards Earth Syst. Sci.* 21, 1531–1550. doi:10.5194/nhess-21-1531-2021

Alvioli, M., Mondini, A. C., Fiorucci, F., Cardinali, M., and Marchesini, I. (2018). Topography-driven satellite imagery analysis for landslide mapping. *Geomatics, Nat. Hazards Risk* 9, 544–567. doi:10.1080/19475705.2018.1458050

Chang, K., Chiang, S. H., and Lei, F. (2008). Analysing the relationship between typhoon-triggered landslides and critical rainfall conditions. *Earth Surf. Process. Landf.* 33 (8), 1261–1271. doi:10.1002/esp.1611

Crozier, M. J. (2005). Multiple-occurrence regional landslide events in New Zealand: Hazard management issues. *Landslides* 2, 247–256. doi:10.1007/s10346-005-0019-7

Dahal, R. K., Hasegawa, S., Nonomura, A., Yamanaka, M., Masuda, T., and Nishino, K. (2009). Failure characteristics of rainfall-induced shallow landslides in granitic terrains of Shikoku Island of Japan. *Environ. Geol.* 56, 1295–1310. doi:10.1007/s00254-008-1228-x

Fell, R., Corominas, J., Bonnard, C., Cascini, L., Leroi, E., and Savage, W. Z. (2008). Guidelines for landslide susceptibility, hazard and risk zoning for land-use planning. *Eng. Geol.* 102, 99–111. doi:10.1016/j.enggeo.2008.03.014

Froude, M. J., and Petley, D. N. (2018). Global fatal landslide occurrence from 2004 to 2016. *Nat. Hazards Earth Syst. Sci.* 18 (8), 2161–2181. doi:10.5194/nhess-18-2161-2018

Gabet, E. J., Burbank, D. W., Putkonen, J. K., Pratt-Sitaula, B. A., and Ojha, T. (2004). Rainfall thresholds for landsliding in the Himalayas of Nepal. *Geomorphology* 63, 131–143. doi:10.1016/j.geomorph.2004.03.011

Guo, C., Xu, Q., Dong, X., Li, W., Zhao, K., Lu, H., et al. (2021). Geohazard recognition and inventory mapping using airborne LiDAR data in complex mountainous areas. *J. Earth Sci.* 32 (5), 1079–1091. doi:10.1007/s12583-021-1467-2

Guo, Z., Shi, Y., Huang, F., Fan, X., and Huang, J. (2021). Landslide susceptibility zonation method based on C5.0 decision tree and K-means cluster algorithms to improve the efficiency of risk management. *Geosci. Front.* 12 (6), 101249. doi:10.1016/j.gsf.2021.101249

Guo, Z., Yin, K., Gui, L., Liu, Q., Huang, F., and Wang, T. (2019). Regional rainfall warning system for landslides with creep deformation in Three Gorges using a statistical black box model. *Sci. Rep.* 9, 8962. doi:10.1038/s41598-019-45403-9

Guo, Z., Yin, K., Liu, Q., Huang, F., Gui, L., and Zhang, G. (2020). Rainfall warning of creeping landslide in Yunyang County of Three Gorges Reservoir based on displacement ratio model. *Earth Sci.* 45 (2), 672–684.

Guzzetti, F., Carrara, A., Cardinali, M., and Reichenbach, P. (1999). Landslide hazard evaluation: A review of current techniques and their application in a multi-scale study, central Italy. *Geomorphology* 31 (1-4), 181–216. doi:10.1016/s0169-555x(99)00078-1

Huang, F., Cao, Z., Guo, J., Jiang, S-H., Li, S., and Guo, Z. (2020). Comparisons of heuristic, general statistical and machine learning models for landslide susceptibility prediction and mapping. *Catena* 191, 104580. doi:10.1016/j.catena.2020.104580

Huang, F., Chen, J., Liu, W., Huang, J., Hong, H., and Chen, W. (2022a). Regional rainfall-induced landslide hazard warning based on landslide susceptibility mapping and a critical rainfall threshold. *Geomorphology* 408, 108236. doi:10.1016/j.geomorph.2022.108236

Huang, F., Tang, C., Jiang, S-H., Liu, W., Chen, N., and Huang, J. (2022b). Influence of heavy rainfall and different slope cutting conditions on stability changes in red clay slopes: A case study in south China. *Environ. Earth Sci.* 81, 384. doi:10.1007/s12665-022-10466-x

Huang, F., Tao, S., Chang, Z., Huang, J., Fan, X., Jiang, S-H., et al. (2021a). Efficient and automatic extraction of slope units based on multi-scale segmentation method for landslide assessments. *Landslides* 18, 3715–3731. doi:10.1007/s10346-021-01756-9

Huang, Y., Xu, C., Zhang, X., Xue, C., and Wang, S. (2021b). An updated database and spatial distribution of landslides triggered by the milin, tibet Mw6.4 earthquake of 18 november 2017. *J. Earth Sci.* 32 (5), 1069–1078. doi:10.1007/s12583-021-1433-z

Hungr, O., Leroueil, S., and Picarelli, L. (2014). The Varnes classification of landslide types, an update. *Landslides* 11 (2), 167–194. doi:10.1007/s10346-013-0436-y

Hürlimann, M., Guo, Z., Carol, P. P., and Medina, V. (2022). Impacts of future climate and land cover changes on landslide susceptibility: Regional scale modelling in the Val d' Aran region (Pyrenees, Spain). *Landslides* 19, 99–118. doi:10.1007/s10346-021-01775-6

Jia, R., Guo, J., and Qi, S. (2019). Landslide hazard during 2000-2016 in Zhejiang Province, the typical subtropical region of Southeast China. *Disaster Adv.* 12 (1), 15–17.

Jiang, S-H., Huang, J., Huang, F., Yang, J., Yao, C., and Zhou, C-B. (2018). Modelling of spatial variability of soil undrained shear strength by conditional random fields for slope reliability analysis. *Appl. Math. Model.* 63, 374–389. doi:10.1016/j.apm.2018.06.030

Khan, Y. A., Lateh, H., Baten, M. A., and Kamil, A. A. (2012). Critical antecedent rainfall conditions for shallow landslides in Chittagong City of Bangladesh. *Environ. Earth Sci.* 67, 97–106. doi:10.1007/s12665-011-1483-0

Kim, H., Lee, J. H., Park, H. J., and Heo, J. H. (2021). Assessment of temporal probability for rainfall-induced landslides based on nonstationary extreme value analysis. *Eng. Geol.* 294, 106372. doi:10.1016/j.enggeo.2021.106372

Kirschbaum, D. B., Adler, R., Hong, Y., and Lerner-Lam, A. (2009). Evaluation of a preliminary satellite-based landslide hazard algorithm using global landslide inventories. *Nat. Hazards Earth Syst. Sci.* 9, 673–686. doi:10.5194/nhess-9-673-2009

Kocaman, S., Tavus, B., Nefeslioglu, H. A., Karakas, G., Gokceoglu, C., and Sarihan, N. H. (2020). Evaluation of floods and landslides triggered by a meteorological catastrophe (ordu, Turkey, August 2018) using optical and radar data. *Geofluids* 1-18, 1–18. doi:10.1155/2020/8830661

Kuradusenge, M., Kumaran, S., and Zennaro, M. (2021). Experimental study of site-specific soil water content and rainfall inducing shallow landslides: Case of gakenke district, Rwanda. *Geofluids* 2021, 7194988. doi:10.1155/2021/7194988

Li, Q., Huang, D., Pei, S., Qian, J., and Wang, M. (2021). Using physical model experiments for hazards assessment of rainfall-induced debris landslides. *J. Earth Sci.* 32 (5), 1113–1128. doi:10.1007/s12583-020-1398-3

Liu, X., Yun, C., Shi, P., and Fang, W. (2012). Debris flow and landslide hazard mapping and risk analysis in China. *Front. Earth Sci.* 6, 306–313. doi:10.1007/s11707-012-0328-9

Liu, Y., Chen, Z., Wang, J., Hu, B., Ye, M., and Xu, S. (2011). Large-scale natural disaster risk scenario analysis: A case study of Wenzhou city, China. *Nat. Hazards (Dordr).* 60, 1287–1298. doi:10.1007/s11069-011-9909-2

Liu, Y., Chen, Z., Wang, J., Xu, S., and Hu, B. (2010). Fifty-year rainfall change and its effect on droughts and floods in Wenzhou, China. *Nat. Hazards (Dordr).* 56, 131–143. doi:10.1007/s11069-010-9556-z

Ma, T., Li, C., Lu, Z., and Bao, Q. (2015). Rainfall intensity-duration thresholds for the initiation of landslides in Zhejiang Province, China. *Geomorphology* 245, 193–206. doi:10.1016/j.geomorph.2015.05.016

Medina, V., Hürlimann, M., Guo, Z., Lloret, A., and Vaunat, J. (2021). Fast physically-based model for rainfall-induced landslide susceptibility assessment at regional scale. *Catena* 201, 105213. doi:10.1016/j.catena.2021.105213

Naidu, S., Sajinkumar, K. S., Oommen, T., Anuja, V. J., Samuel, R. A., and Muraleedharan, C. (2018). Early warning system for shallow landslides using rainfall threshold and slope stability analysis. *Geosci. Front.* 9, 1871–1882. doi:10.1016/j.gsf.2017.10.008

Nolasco-Javier, D., Kumar, L., and Tengonciang, A. M. P. (2015). Rapid appraisal of rainfall threshold and selected landslides in Baguio, Philippines. *Nat. Hazards (Dordr).* 78, 1587–1607. doi:10.1007/s11069-015-1790-y

Peng, J., Wang, S., Wang, Q., Zhuang, J., Huang, W., Zhu, X., et al. (2019). Distribution and genetic types of loess landslides in China. *J. Asian Earth Sci.* 170, 329–350. doi:10.1016/j.jseaes.2018.11.015

Prakash, N., Manconi, A., and Loew, S. (2020). Mapping landslides on EO data: Performance of deep learning models vs. Traditional machine learning models. *Remote Sens.* 12, 346. doi:10.3390/rs12030346

Rahardjo, H., Leong, E. C., and Rezaur, R. B. (2008). Effect of antecedent rainfall on pore-water pressure distribution characteristics in residual soil slopes under tropical rainfall. *Hydrol. Process.* 22, 506–523. doi:10.1002/hyp.6880

Robbins, J. C. (2016). A probabilistic approach for assessing landslide-triggering event rainfall in Papua New Guinea, using TRMM satellite precipitation estimates. *J. Hydrology* 541, 296–309. doi:10.1016/j.jhydrol.2016.06.052

Santangelo, M., Cardinali, M., Rossi, M., Mondini, A. C., and Guzzetti, F. (2010). Remote landslide mapping using a laser rangefinder binocular and GPS. *Nat. Hazards Earth Syst. Sci.* 10 (12), 2539–2546. doi:10.5194/nhess-10-2539-2010

Tseng, C. W., Song, C. E., Wang, S. F., Chen, Y. C., Tu, J. Y., Yang, C. J., et al. (2020). Application of high-resolution radar rain data to the predictive analysis of landslide susceptibility under climate change in the laonong watershed, taiwan. *Remote Sens.* 12, 3855. doi:10.3390/rs12233855

Varnes, D. J. (1978). "Slope movement types and processes," in *Landslides, analysis and control, special report 176: Transportation research board.* Editors R. L. Schuster and R. J. Krizek (Washington, DC: National Academy of Sciences), 11–33.

Wang, D. J., Tang, H. M., Zhang, Y. H., Chang, D. L., and Huang, L. (2017). An improved approach for evaluating the time-dependent stability of colluvial landslides during intense rainfall. *Environ. Earth Sci.* 76, 321. doi:10.1007/s12665-017-6639-0

Wang, Y., and Yin, K. (2018). Typhoon-triggered debris flow hazard prediction in southeast mountain area in Zhejiang Province. *IOP Conf. Ser. Earth Environ. Sci.* 170 (2), 022135. doi:10.1088/1755-1315/170/2/022135

Webster, P. J., Magaña, V. O., Palmer, T. N., Shukla, J., Tomas, R. A., Yanai, M., et al. (1998). Monsoons: Processes, predictability, and the prospects for prediction. *J. Geophys. Res.* 103, 14451–14510.

Wei, Z., Shang, Y., Zhao, Y., Pan, P., and Jiang, Y. (2017). Rainfall threshold for initiation of channelized debris flows in a small catchment based on in-site measurement. *Eng. Geol.* 217, 23–34. doi:10.1016/j.enggeo.2016.12.003

Wei, Z., Xu, Y., Sun, H., Xie, W., and Wu, G. (2018). Predicting the occurrence of channelized debris flow by an integrated cascading model: A case study of a small debris flow-prone catchment in Zhejiang Province, China. *Geomorphology* 308, 78–90. doi:10.1016/j.geomorph.2018.01.027

Wu, W., Xu, C., Wang, X., Tian, Y., and Deng, F. (2020). Landslides triggered by the 3 August 2014 ludian (China) mw 6.2 earthquake: An updated inventory and analysis of their spatial distribution. *J. Earth Sci.* 31 (4), 853–866. doi:10.1007/s12583-020-1297-7

Wu, Y., Chen, L., Cheng, C., Yin, K., and Torok, A. (2014). GIS-based landslide hazard predicting system and its real-time test during a typhoon, Zhejiang Province, Southeast China. *Eng. Geol.* 175, 9–21. doi:10.1016/j.enggeo.2014.03.005

Xu, Q., Liu, H., Ran, J., Li, W., and Sun, X. (2016). Field monitoring of groundwater responses to heavy rainfalls and the early warning of the Kualiangzi landslide in Sichuan Basin, southwestern China. *Landslides* 13, 1555–1570. doi:10.1007/s10346-016-0717-3

Yin, Y., Wang, L., Zhang, W., and Dai, Z. (2022). Research on the collapse process of a thick-layer dangerous rock on the reservoir bank. *Bull. Eng. Geol. Environ.* 81 (3), 109. doi:10.1007/s10064-022-02618-x

Zhang, Y., Guo, J., and Che, Z. (2014). Discussion on evaluating the vulnerability of storm surge hazard bearing bodies in the coastal areas of Wenzhou. *Front. Earth Sci.* 9, 300–307. doi:10.1007/s11707-014-0453-8

Zhou, Z., Zhang, J., Ning, F., Luo, Y., Chong, L., and Sun, K. (2020). Large-scale test model of the progressive deformation and failure of cracked soil slopes. *J. Earth Sci.* 31 (6), 1097–1108. doi:10.1007/s12583-020-1342-6

Zhuang, Y., Xing, A., Jiang, Y., Sun, Q., Yan, J., and Zhang, Y. (2022). Typhoon, rainfall and trees jointly cause landslides in coastal regions. *Eng. Geol.* 298, 106561. doi:10.1016/j.enggeo.2022.106561